Solubilization and Controlled Release of a Hydrophobic Drug Using Novel Micelle-Forming ABC Triblock Copolymers

Yiqing Tang, Shiyong Y. Liu, Steven P. Armes, and Norman C. Billingham*

Department of Chemistry, University of Sussex, Falmer, Brighton BN1 9QJ, United Kingdom

Received April 1, 2003; Revised Manuscript Received August 18, 2003

Amphiphilic ABC triblock copolymers composed of monomethoxy-capped poly(ethylene glycol) (MPEG), poly(2-(dimethylamino)ethyl methacrylate) (DMA), and poly(2-(diethylamino)ethyl methacrylate) (DEA) have been synthesized by atom transfer radical polymerization (ATRP). These copolymers dissolve molecularly in acidic aqueous media at room temperature due to protonation of the tertiary amine groups on the DMA and DEA residues. On adjusting the pH with base, micellization occurred at pH 8, with the water-insoluble, deprotonated DEA block forming the hydrophobic cores and the MPEG and DMA blocks forming the hydrophilic micellar coronas and inner shells, respectively. This pH-induced micellization has been exploited to develop a solvent-free protocol for drug loading. A model hydrophobic drug, dipyridamole (DIP), which dissolves in acid but is insoluble above pH 5.8, was incorporated into the micelles by increasing the pH of an aqueous drug/copolymer mixture to 9. Both the empty and the drug-loaded micelles were characterized by dynamic light scattering and fluorescence studies. The interaction of both pyrene and DIP with the MPEG−DMA−DEA micelles was studied by fluorescence; both compounds had relatively high partition coefficients into the micelles, 4.5×10^5 and 1.5×10^4, respectively. Intensity-average micelle diameters ranged from 20 to 90 nm, depending on the polymer composition and concentration. Shorter MPEG blocks ($M_n = 2000$) produced larger micelles than longer MPEG blocks ($M_n = 5000$) due to the shift in the hydrophilic−hydrophobic balance of the copolymer. Transmission electron microscopy studies of the drug-loaded micelles indicated spherical morphologies and reasonably uniform particle size distributions, which is in marked contrast to the needlelike morphology observed for pure DIP in the absence of the copolymer. Experiments on controlled release demonstrated that DIP-loaded MPEG−DMA−DEA micelles act as a drug carrier, giving slow release to the surrounding solution over a period of days. Rapid release can be triggered by reducing the pH to reverse the micellization.

Introduction

Polymeric micelles have been studied extensively because of their applications in medicine, in drug delivery and diagnostic imaging,[1] and in environmental science, to enhance solubility of insoluble organic substances.[2] Micelles are usually composed of a hydrophobic core and a hydrophilic corona. This core−corona structure is of great importance for solubilizing water-insoluble compounds; the hydrophobic core is able to provide a suitable microenvironment for the "active", and the hydrophilic corona acts as a steric stabilizer for the hydrophobic region in the aqueous environment. Inter-polyelectrolyte micelles, where the micellar core is formed by a polyelectrolyte complexed with an ionic drug or protein through electrostatic interaction, are of interest for the delivery of DNA, peptides and proteins.[3]

There has been particular interest in self-assembled micelles with poly(ethylene glycol) (PEG) or poly(ethylene oxide) (PEO) as the corona-forming block because of its excellent biocompatibility, long blood circulation time, and nontoxicity.[4] A number of PEG-based block copolymers have been explored for the purpose of drug delivery and targeting. Micelles from PEO−poly(propylene oxide)−PEO triblock copolymers (Pluronic), in which poly(propylene oxide) acts as the hydrophobic core, have been investigated by many groups, for neuroleptic targeting and cytotoxic drug delivery.[5] Poly(γ-benzyl-L-glutamate), poly(β-benzyl-L-aspartate), polycaprolactone, poly(*N*-isopropylacrylamide), polylactide, and polylysine have also been prepared in combination with PEG or PEO−PPO−PEO for drug delivery studies.[6−9]

Drug-loading capacity, drug-micelle stability, and release kinetics are largely determined by the compatibility of the solubilized drug and the core-forming block.[1c] Theoretical studies of the mechanism of solubilization suggested initial exclusion of water molecules and hydrophilic blocks from the micelle cores, followed by an accumulation of hydrophobic drug, which can solubilize the hydrophobic blocks.[10] Further solubilization could result in a region of pure drug in the inner core, whose surface is decorated by the adsorbed hydrophobic blocks. Meanwhile, interactions (if any) between the drug and the hydrophilic coronal block, and the interfacial tension between drug, solvent, and water, can also affect the drug solubilization behavior.

Depending on the method of micelle preparation, there are different protocols for the incorporation of drugs into micelles: dissolution and dialysis are the most common. Both

* To whom correspondence should be addressed. E-mail: n.billingham@sussex.ac.uk.

10.1021/bm030026t CCC: $25.00
Published on Web 10/09/2003

protocols involve dissolution of either the drug or the copolymer in a volatile organic solvent, with either solvent evaporation or dialysis being used to remove the solvent after loading has been achieved. Recently, a solvent-free protocol for the preparation of block copolymer micelles in aqueous solution by adjusting the solution pH has been reported by several groups.[11−13] In each case, one of the blocks is a weak cationic polyelectrolyte that is soluble at low pH but becomes insoluble at higher pH. This tunable block forms the micelle cores, whereas a permanently hydrophilic, usually PEG-based, block forms the coronas. In principle, such pH-induced micellization could be exploited for the triggered release of hydrophobic drugs in a low pH environment (e.g., in the gut or within a cell).

Recently, we reported the reversible formation of block copolymer micelles using either methoxy-capped poly(ethylene glycol) or poly(2-(dimethylamino)ethyl methacrylate) [DMA] as the hydrophilic block, combined with poly(2-(diethylamino)ethyl methacrylate) [DEA], poly(2-(diisopropylamino)ethyl methacrylate) [DPA], or poly(2-(*N*-morpholino)ethyl methacrylate) [MEMA] as the hydrophobic block. In each case, micellization was fully reversible and depended on the solution pH, temperature, and/or salt concentration.[14] Living polymerization techniques such as atom transfer radical polymerization (ATRP) and group transfer polymerization (GTP) were used to prepare these block copolymers with predetermined degrees of polymerization and low polydispersities ($M_w/M_n < 1.1-1.3$).[15] In particular, a novel triblock copolymer, MPEG−DMA−DEA, was synthesized which dissolved molecularly at low pH and formed micelles at around pH 7−8 due to deprotonation of the DEA block. Selective cross-linking of the central DMA block was achieved using the bifunctional quaternizing reagent, 1,2-bis(2-iodoethoxy)ethane (BIEE),[16] leading to covalently stabilized shell cross-linked micelles which remained intact in acidic solution.

The aim of the present work was to use ATRP to prepare a series of ABC triblock copolymers comprising methoxy-capped poly(ethylene glycol)-*b*-poly(2-(dimethylamino)ethyl methacrylate)-*b*-poly(2-(diethylamino)ethyl methacrylate) (MPEG−DMA−DEA). The effect of varying the triblock composition on the micelle diameter was studied using dynamic light scattering (DLS). Using dipyridamole (DIP) as a model drug, we have evaluated a protocol for its solvent-free loading into the MPEG−DMA−DEA micelles that are formed at pH 8. Both pH-triggered solubilization and release of DIP were demonstrated and synthesis−structure−property relationships were examined. Finally, the size and morphology of the drug-loaded micelles were investigated by transmission electron microscopy (TEM) and DLS.

Experimental Section

Materials. Monomethoxy-capped poly(ethylene glycol) (MPEG, $M_n = 2000$, $M_w/M_n = 1.04$; and $M_n = 5000$, $M_w/M_n = 1.07$) were gifts from Laporte. 2-Bromoisobutyryl bromide, triethylamine, copper(I) bromide (CuBr), 2,2′-bipyridine (bpy), 2-(dimethylamino)ethyl methacrylate (DMA), 2-(diethylamino)ethyl methacrylate (DEA), pyrene, and DIP (Scheme 1) were purchased from Aldrich. The DMA and DEA monomers were each passed through a basic alumina column before use to remove the inhibitor. Toluene was purified and dried by azeotropic distillation. Water used in micelle studies was deionized then doubly distilled (Fistreem Cyclone still).

Scheme 1

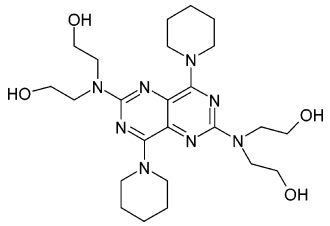

Synthesis of Macroinitiators. The PEG macro-initiators were prepared according to a literature procedure.[15] MPEG ($M_n = 2000$, 10.0 g, 5 mmol) and triethylamine (0.81 g, 8 mmol) were dissolved in 200 mL of toluene at room temperature. 2-Bromoisobutyryl bromide (1.84 g, 8 mmol) was added dropwise, and the solution was stirred overnight. The reaction mixture was then filtered to separate the precipitated hydrobromide salt, and toluene was removed using a rotary evaporator. The resulting white product was dissolved in 1% Na_2CO_3 solution and extracted using dichloromethane. The collected organic layer was dried over $MgSO_4$, and the solvent was removed under vacuum.

Synthesis of MPEG-DMA-DEA Triblock Copolymer. Poly[ethylene glycol-*b*-2-(dimethylamino)ethyl methacrylate-*b*-2-(diethylamino)ethyl methacrylate] (MPEG−DMA−DEA) was synthesized using ATRP. In a typical synthesis, the preweighed PEG2000 macro-initiator (0.5 g, 0.233 mmol) and DMA (1.57 g, 10 mmol) were dissolved in 2 mL of doubly distilled water in a Schlenk tube, and the solution was degassed by a single freeze−thaw−pump cycle. On warming to room temperature, the catalyst (CuBr, 0.033 g, 0.233 mmol) and ligand (2,2′-bipyridine, 0.073 g, 0.466 mmol) were added to this solution to start the polymerization under a nitrogen atmosphere. At the end of the first-stage polymerization of DMA, a degassed methanolic solution of DEA (4.32 g, 23.3 mmol) was added, and the second-stage polymerization allowed to proceed overnight. The polymerization was terminated by exposing the reaction solution to air, leading to aerial oxidation of the brown Cu(I) catalyst. The blue reaction mixture was then diluted with methanol and passed through a silica column to remove the spent Cu(II) complex. The colorless polymer was collected after removal of methanol by freeze-drying from aqueous solution. As described in our previous full report of the synthesis,[16] this approach gives polymers with low polydispersities (measured by gel permeation chromatography (GPC)) and chain lengths (measured by ^{1}H NMR spectroscopy) in good agreement with those predicted from the monomer:initiator ratios.

Preparation of Micelles with or without Drug. The MPEG−DMA−DEA copolymer was dissolved at pH 2 by adding HCl (1 M) to the aqueous solution. Micelles were prepared by adjusting this copolymer solution to pH 8−9

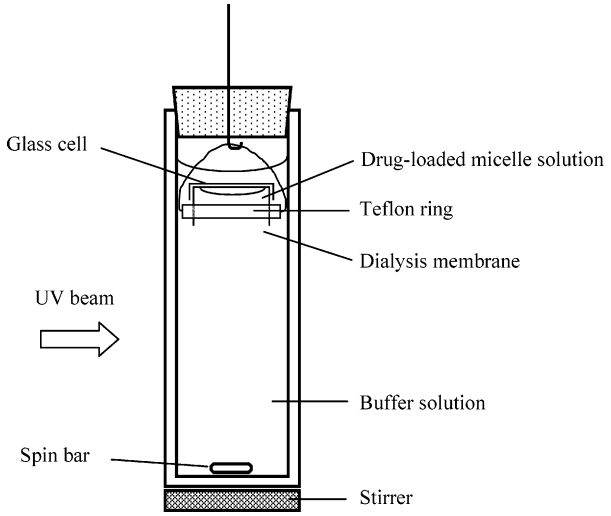

Figure 1. Schematic of set up for in situ UV measurement of drug release from micelles.

with NaOH (2 M). Drug-loaded micelles were prepared by dissolving DIP in the copolymer solution at pH 2, followed by the addition of NaOH to form drug-loaded micelles at pH 8−9. In principle, an alternative method to prepare the drug-loaded micelles is to mix freshly precipitated DIP at pH 8 with the micellar solution at pH 8−9, whereupon the precipitate becomes solubilized. In this paper, the former protocol was used for drug loading unless otherwise specified.

Fluorescence Spectroscopy The fluorescence spectra of DIP and pyrene in aqueous micellar solutions were obtained at 20 °C using a Cary Eclipse Fluorescence spectrophotometer. Fluorescence emission spectra were recorded at λ_{ex} = 415 nm for DIP partition measurements. To obtain a significant fluorescence intensity change, a solution of DIP in KCl/NaOH buffer was prepared at pH 12.7, which is above the pK_1 of DIP (12.5).[17] The concentration of DIP in the buffer was 5×10^{-6} M. Aliquots of 1 g L^{-1} MPEG−DMA−DEA stock solution were then added directly into the DIP buffer solution in the fluorescence cell.

For partition experiments using pyrene, λ_{ex} was set to 333 nm for the observation of emission spectra and λ_{em} was set at 373 nm for the observation of excitation spectra. Pyrene solutions were prepared by adding known amounts of pyrene dissolved in acetone into dry volumetric flasks. After evaporation of the acetone, copolymer solutions were added (at pH 12.7 for partition experiments) to produce a final pyrene concentration of 6.0×10^{-7} M.

Determination of Drug Loading in the Micelles. Drug-loaded micelles were dissolved in a pH 3 citric acid/sodium citrate buffer, to reverse the micellization, and the concentration of DIP was determined either by UV spectroscopy or by fluorescence measurements. The loading content is expressed as the mass of loaded drug per unit weight of copolymer.

In Vitro Drug Release. Drug release experiments were carried out by using a quartz cuvette as a diffusion cell, in which the released drug concentration was monitored in situ by UV spectroscopy. Figure 1 shows the setup for the direct measurement of drug release from micelles contained in a small cell separated from the surrounding solution by a dialysis membrane with molecular weight cutoff (MWCO) of 15 000. The sample cell, holding 0.09 g, of 0.5 g L^{-1} micelle solution with 20 w/w % of entrapped drug was immersed in 3.0 g phosphate buffer solution (PBS) (pH 7.4) at 37 °C, which was stirred by a spin bar. Before an autoscanning run, the absorbance was zeroed with PBS at 291 nm. The release curve was recorded immediately after the glass cell was immersed in the buffer. To maintain a sink condition for the release experiments, only the first three or 4 h of release were monitored. As controls, experiments for pH effects were designed as the release of drug without micelles into pH 3 buffer, in which the amount of drug (at pH 3) was equivalent to 20 w/w % of drug in 0.09 g, 0.5 g L^{-1} of micelle solution and the release of drug with micelle (at pH 8) to pH 3 buffer. In the pH 3 buffer solution, the UV absorbance was measured at 284 nm.

The release monitoring performance of this setup was compared with the data obtained from a dialysis bag (MWCO 15 000), with 5 mL of 0.5 g L^{-1} micelle solution loaded with 20% drug, into 50 mL of PBS (pH 7.4) at 37 °C. Samples (1 mL) were taken from the buffer at defined time intervals and assayed by UV spectroscopy at 291 nm. Meanwhile, the sampled volume was immediately replaced with fresh PBS (1 mL). Cumulative release is expressed as the total percentage of available drug released through the dialysis membrane over time.

Characterization Techniques and Instrumentation. All ^{1}H NMR spectra were recorded in $CDCl_3$ at 300 MHz, using a Bruker Avance DPX 300 spectrometer. Molecular weights and molecular weight distributions were determined using a gel permeation chromatography (GPC) instrument (PLgel 3 μm MIXED-E 300 × 7.5 mm column, THF eluent, PMMA calibration standards, refractive index detector). DLS measurements were carried out using a Brookhaven instrument equipped with a solid-state laser (125 mW, λ = 532 nm) and a BI-9000At digital correlator. The DLS measurements were made at a fixed angle of 90°, and the temperature was controlled at 20 °C. The data were analyzed using the manufacturer's software for the CUMULANTS method. The effective diameter and polydispersity were determined from the first and second cumulants of a Taylor series which is the expanded exponential part of the normalized autocorrelation function. The validity of this approach depends on a low contribution from higher-order terms, which is generally the case for polydispersities below 0.3, as was always the case in this study.

UV−visible absorption spectra were recorded on a Perkin-Elmer UV/vis Lambda 2S spectrophotometer. Transmission electron microscopy (TEM) studies were carried out on a Hitachi 7100 instrument. TEM samples were prepared by contacting the aqueous micelle solution onto TEM grids (Agar Scientific Limited), followed by drying at ambient temperature.

Results and Discussion

Triblock Copolymer Synthesis and Characterization. ATRP is very tolerant of monomer functionality, and if a

Table 1. Characteristics of Synthesized Triblock Copolymers

	PEG chain	DEA content[a] (mol %)	M_n[b]	M_w/M_n
$MPEG_{45}-DMA_{47}-DEA_{120}$	2000	56.6	34 100	1.20
$MPEG_{45}-DMA_{50}-DEA_{95}$	2000	50.0	29 500	1.24
$MPEG_{113}-DMA_{40}-DEA_{125}$	5000	45.3	38 900	1.34
$MPEG_{113}-DMA_{38}-DEA_{86}$	5000	36.3	35 900	1.19

[a] Determined from ^{1}H NMR. [b] Measured by THF GPC.

macro-initiator route is used, it can be very convenient for the preparation of a wide range of amphiphilic polymeric surfactants.[15,16] Detailed studies have been carried out on the polymerization of DMA and DEA using various PEG-based macroinitiators.[16,18] Following previous work,[16] the "one-pot" synthesis of $MPEG_{45}-DMA_{50}-DEA_{95}$ and $MPEG_{45}-DMA_{47}-DEA_{120}$ was achieved, with somewhat higher target degrees of polymerization (DP) for the DEA block so as to produce more hydrophobic micelle cores and higher micelle aggregation numbers and maximize the drug-loading capacity of the micelles. The homopolymerization of DMA using the $PEG_{45}-Br$ macro-initiator was very rapid in water and was essentially complete (>98% conversion) within 30 min at 20 °C. Subsequent block copolymerization of the DEA (added as a methanol solution to ensure miscibility) was rather slower, but high conversions were achieved after 16 h at 20 °C.The polydispersity indices of $MPEG_{45}-DMA_{50}-DEA_{95}$ and $MPEG_{45}-DMA_{47}-DEA_{120}$ triblock copolymers were 1.24 and 1.20, respectively, indicating that the polymerizations were fairly well-controlled. Table 1 summarizes the characterization data for the four copolymers used in micelle studies. The DP of each block was determined by ^{1}H NMR analysis using the PEG block as an "end-group". The overall number-average molecular weights (Mn) of the copolymers ranged from 29 000 to 39 000. Two copolymers were based on a shorter MPEG (DP = 45) and two on a longer MPEG (DP = 113). In both cases, the DMA block length was kept approximately constant and the DEA block length was varied. The purpose of the water-soluble DMA block in these copolymers is to allow shell cross-linking using BIEE and hence examination of the effect of degree of cross-linking on the kinetics of release from the micelles. However, this does not form part of the present study, thus the PEG and DMA segments are considered as an integrated hydrophilic block.[15,14a] Hence, for example, the relatively high DEA content of the $MPEG_{45}-DMA_{47}-DEA_{120}$ copolymer was expected to produce somewhat larger micelles compared to the relatively hydrophilic $MPEG_{113}-DMA_{50}-DEA_{95}$ copolymer (see Table 1).

Micelle Formation by Adjusting the Solution pH. Because the MPEG−DMA−DEA triblock copolymers have hydrophilic and hydrophobic blocks in the same chain, micellar self-assembly can occur under appropriate circumstances. In particular, because of the basic amine groups in the DMA and DEA blocks, self-assembly can be controlled by changing the solution pH.[14b,19]

Fluorescence spectroscopy is a well-established method to detect micelle formation by using a molecular probe whose emission and excitation spectra are sensitive to the surrounding environment, pyrene being a good example.[20] Figure 2 shows the changes of pyrene emission and excitation spectra with pH from 2.5 to 9 in the presence of 0.5 g L^{-1} $MPEG_{45}-DMA_{47}-DEA_{120}$. At pH 2.5, the triblock copolymer exists as water-soluble unimers due to the complete protonation of the amine groups on the DMA and DEA blocks. Thus, it shows the typical emission spectrum of pyrene in water in Figure 2a (solid line), where the intensity ratio of the first and third vibrational bands, I_1/I_3, is about 1.80. As the solution pH is raised to around 9, I_1/I_3 decreases to 1.30 as shown in Figure 2a. Meanwhile, as shown in Figure 2b, the pyrene excitation spectrum exhibits a large red-shift. Both changes indicate that the microenvironment of pyrene becomes hydrophobic, which confirms the formation of micelles when the pH is increased from 2.5 to 9. Thus, the deprotonation of the amine groups on DEA and DMA induces aggregation of the water-insoluble blocks, and the cationic copolymer chains become amphiphilic. Figure 3, shows how the I_1/I_3 ratio for pyrene changes with pH and copolymer concentration for the fluorescence spectra of pyrene in the $MPEG_{45}-DMA_{47}-DEA_{120}$ copolymer solutions. The curves show that micellization is complete above pH 7.3, and the slight decrease in the I_1/I_3 ratio with pH

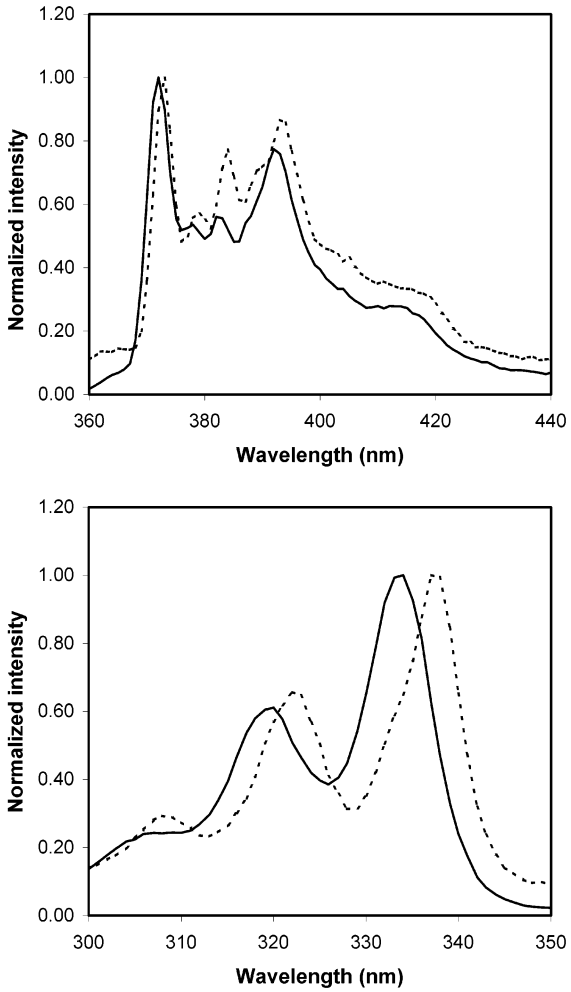

Figure 2. (a) Emission spectra of pyrene in the presence of 0.5 g L^{-1} $MPEG_{45}-DMA_{47}-DEA_{120}$ unimers (solid line, pH 2.5) and micelles (dotted line, pH 9), λ_{ex} = 333 nm. (b) Excitation spectra of pyrene in the presence of 0.5 g L^{-1} $MPEG_{45}-DMA_{47}-DEA_{120}$ unimers and micelles, λ_{ex} = 373 nm.

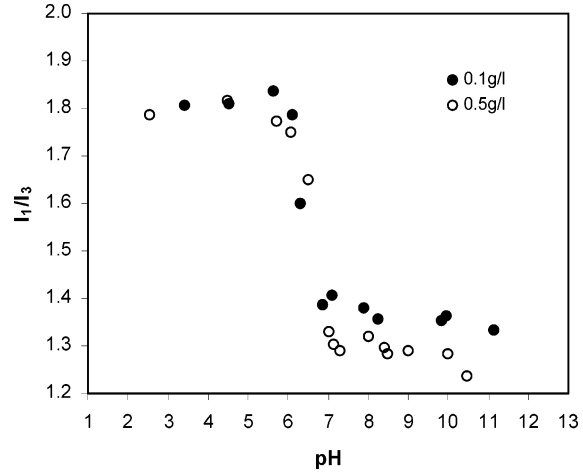

Figure 3. I_1/I_3 intensity ratios from pyrene emission spectra of 0.1 (closed circle) and 0.5 g L^{-1} (open circle) $MPEG_{45}-DMA_{47}-DEA_{120}$ change with pH, $\lambda_{ex} = 333$ nm.

suggests continuously increasing hydrophobicity in the core. Both phenomena are consistent with previous studies,[16,19] in which it was suggested that micellization occurred at pH 7.1−7.3, meanwhile, a loose micelle structure was observed from pH 7.3 to 8.5 and attributed to the partial deprotonation of the DMA and DEA blocks. I_1/I_3 curves for solutions of different copolymer concentrations are also compared in Figure 3. The lower I_1/I_3 value obtained for a 0.5 g L^{-1} solution of $MPEG_{45}-DMA_{47}-DEA_{120}$ compared to a 0.1 g L^{-1} solution indicates a more hydrophobic micelle core in the former case. It seems reasonable to anticipate that more concentrated copolymer solutions would lead to more hydrophobic blocks and bigger micellar aggregates. This hypothesis was confirmed by DLS measurements for the $MPEG_{45}-DMA_{47}-DEA_{120}$ copolymer, which are discussed later.

Partitioning of Pyrene and DIP into Micelles. Addition of MPEG−DMA−DEA copolymer solutions to buffered solutions of either pyrene or DIP at the appropriate pH leads to micelle formation. Once micelles are present, hydrophobic molecules such as DIP and pyrene can be expected to be partitioned between the bulk solution and the micelle cores, and this partitioning can be measured if there is a measurable change in the spectroscopic properties of the probe molecule with the change in its local environment.

Figure 4 shows how the I_{338}/I_{332} ratio for pyrene fluorescence varies with copolymer concentration for a 6×10^{-7} M pyrene solution in solutions containing MPEG−DMA−DEA copolymers. The data show that the proportion of the pyrene which experiences a hydrophobic environment increases as the polymer concentration increases.

For partitioning of a probe molecule between micelles and solution, with a partition coefficient K, it is easy to show[21] that the fraction of the probe molecule which is present in the micelle cores is given by

$$\frac{1}{F} = \frac{V_s}{KV_m} + 1 \qquad (1)$$

where V_s and V_m are the volumes of micelles and solvent, respectively. It is thus obvious that F will increase as the concentration of micelles increases.

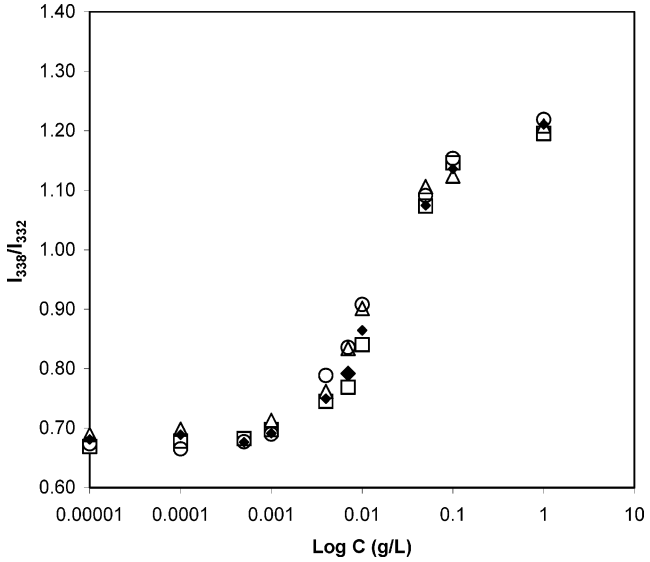

Figure 4. I_{338}/I_{332} intensity ratios from pyrene excitation spectra of MPEG-DMA-DEA copolymers as a function of concentration at pH 9, $\lambda_{em} = 373$ nm. $MPEG_{45}-DMA_{50}-DEA_{95}$ (◆); $MPEG_{45}-DMA_{47}-DEA_{120}$ (○); $MPEG_{113}-DMA_{38}-DEA_{86}$ (□); $MPEG_{113}-DMA_{40}-DEA_{125}$ (△).

If the weight concentration of polymer in the solution is C, then eq 1 can be written as

$$\frac{1}{F} = 1 + \frac{\rho}{K\alpha}\frac{1}{C} \qquad (2)$$

where ρ is the density of the micelle core (taken as the bulk density of the polymer and in this case set equal to 1 g cm^{-3}) and α is the fraction of the polymer which is core forming (calculated from the composition)

The fluorescence intensity from a solution of probe at a fixed concentration is I_{min} in the absence of micelles and I_{max} at high C. If it is assumed that I_{max} corresponds to the situation where essentially all of the probe is in the micelle cores, then it can be shown[21] that eq 2 becomes

$$\frac{1}{I - I_{min}} = \frac{1}{(I_{max} - I_{min})} + \frac{\rho}{K\alpha C(I_{max} - I_{min})} \qquad (3)$$

where I is the fluorescence intensity, measured at a polymer concentration C, so that K can be determined from the slope and intercept of a plot of $1/(I-I_{min})$ against $1/[M]$.

To test eq 3 for our systems, fluorescence data were obtained for both pyrene and DIP. In these systems, we found that the absolute fluorescence intensity observed for pyrene decreased with copolymer concentration, and a red shift was observed in the excitation spectra. DIP contains both aromatic and aliphatic nitrogen atoms and the corresponding pK_a values are 5.7 and 12.5, respectively. The quantum yield of fluorescence of DIP is significantly reduced at low pH (< pH 5.7) and also at high pH (> pH 12.5)[17a] In initial studies of DIP partitioning, we found that the fluorescence intensity of DIP was essentially unchanged as the copolymer concentration was increased at neutral pH. This observation is consistent with literature reports[17a] and was attributed to the relatively high quantum yield of DIP fluorescence. To obtain a large change in the fluorescence intensity, DIP was

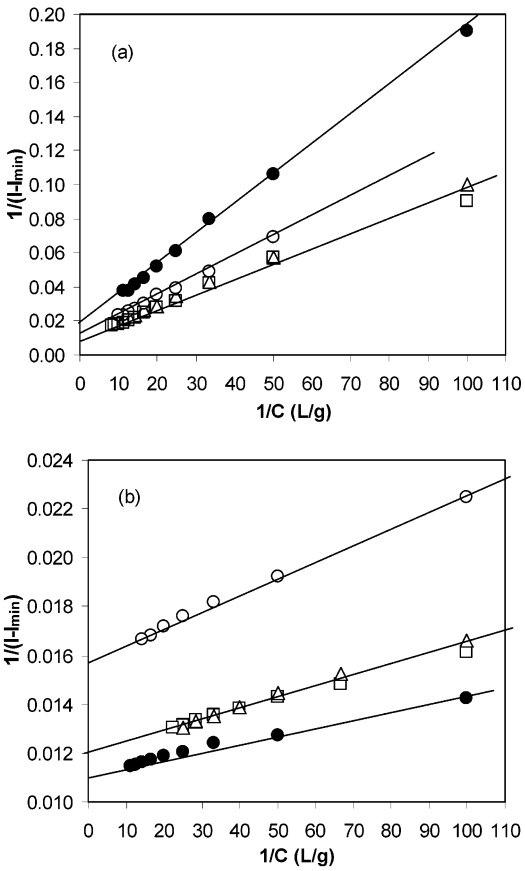

Figure 5. Determination of DIP and pyrene partition coefficients from the variation of fluorescence intensity with the concentration of MPEG−DMA−DEA copolymers in pH 12.7 buffer. The copolymer micelles are $MPEG_{45}-DMA_{47}-DEA_{120}$ (●), $MPEG_{45}-DMA_{50}-DEA_{95}$ (□), $MPEG_{113}-DMA_{38}-DEA_{86}$ (ctuor), $MPEG_{113}-DMA_{38}-DEA_{125}$ (○). In (a) the fluorescence intensity of DIP was derived from emission spectra at 480 nm with $\lambda_{ex} = 415$ nm and in (b) the fluorescence intensity of pyrene was derived from excitation spectra at 333 nm with $\lambda_{em} = 373$ nm. Concentration of DIP is 5.0×10^{-6} M, and concentration of pyrene is 6.0×10^{-7} M.

Table 2. Probe Partition Coefficients of MPEG−DMA−DEA Micelles

polymer	*K* of DIP	*K* of pyrene
$MPEG_{45}-DMA_{47}-DEA_{120}$	$1.5 \pm 0.7 \times 10^4$	$5.4 \pm 1.2 \times 10^5$
$MPEG_{45}-DMA_{50}-DEA_{95}$	$1.3 \pm 0.7 \times 10^4$	$4.8 \pm 1.2 \times 10^5$
$MPEG_{113}-DMA_{40}-DEA_{125}$	$1.5 \pm 0.7 \times 10^4$	$3.4 \pm 1.2 \times 10^5$
$MPEG_{113}-DMA_{38}-DEA_{86}$	$2.2 \pm 0.7 \times 10^4$	$5.2 \pm 1.2 \times 10^5$

dissolved in a pH 12.7 buffer at a concentration of 5×10^{-6} M; under these conditions, the DIP was fully deprotonated and the change in the local environment of the DIP probe was indicated by an increase of fluorescence intensity with copolymer concentration and a blue shift in the DIP emission spectra. As a comparison, a 6×10^{-7} M pyrene solution in the pH 12.7 buffer was also prepared.

Figure 5 shows the plot of fluorescence intensities for DIP and pyrene as a function of the copolymer concentration in the coordinates of eq 3. Good straight lines are obtained and the derived partition coefficients are listed in Table 2.

These *K* values are fairly typical of micellar core partitioning and demonstrate the strong partitioning of the hydrophobic molecules into the micelle cores. For example, Koslov et al.[22] report values of 10^2-10^3, depending on hydrophobic

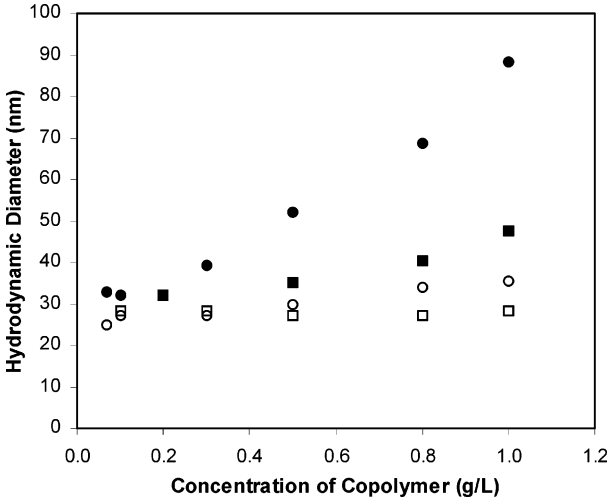

Figure 6. Effective diameter change with micellar concentration from dynamic light scattering measurements at pH 9 (20 °C). Samples with short PEG2000 chain [$MPEG_{45}-DMA_{50}-DEA_{95}$ (○) and $MPEG_{45}-DMA_{47}-DEA_{120}$ (●)] show an increased diameter with concentration due to micellar aggregation. $MPEG_{113}-DMA_{38}-DEA_{86}$ (□) and $MPEG_{113}-DMA_{40}-DEA_{125}$ (■) with longer PEG5000 chain show small diameter change with concentration.

block length, for the partitioning of pyrene from water into pluronic micelles. The variation of *K* with the copolymer structure is too small to draw any conclusions. However, the pyrene partition coefficient in all of the copolymer micelles is significantly higher than that of DIP, because pyrene is more hydrophobic than DIP.

In principle, data such as those in Figure 4 might be interpreted in terms of the critical micelle concentration, rather than as partitioning between the solution and preexisting micelles.[20] Although it is difficult to give absolute proof that micelles are present at all points in the concentration range studied, we believe that this is the case. The micelle solutions used here were prepared at high concentrations and high pH then diluted over the range studied. At high pH, these micelles are effectively "locked" by the dehydration of the core blocks and the DEA block is undetectable by NMR experiments, confirming its immobility. Direct evidence for a partitioning model is provided by the fact that the point of inflection in Figure 4 shifts by an order of magnitude in concentration when DIP is substituted for pyrene (reflected in the derived values of *K*); it is unlikely that changing the probe molecule would have such a large effect on the cmc. We looked very carefully at data generated at low concentrations but were unable within experimental error to detect a break corresponding to a cmc, as reported by Wilhelm et al.[20]

Effect of Copolymer Concentration on Micelle Size. Figure 6 shows the change in the intensity-average micelle diameter, as measured by DLS, with copolymer concentration. In the low concentration range ($0.07-0.10$ g L^{-1}), the micelles formed by these triblock copolymers have diameters ranging between 25 and 35 nm. With increased copolymer concentration, the size of $MPEG_{113}-DMA_{38}-DEA_{125}$ micelles only increased from 32 to 48 nm, although it has the longest chain length of all the copolymers; $MPEG_{45}-DMA_{50}-DEA_{95}$ and $MPEG_{113}-DMA_{38}-DEA_{86}$ micelles show a similar trend, with only very small or near zero

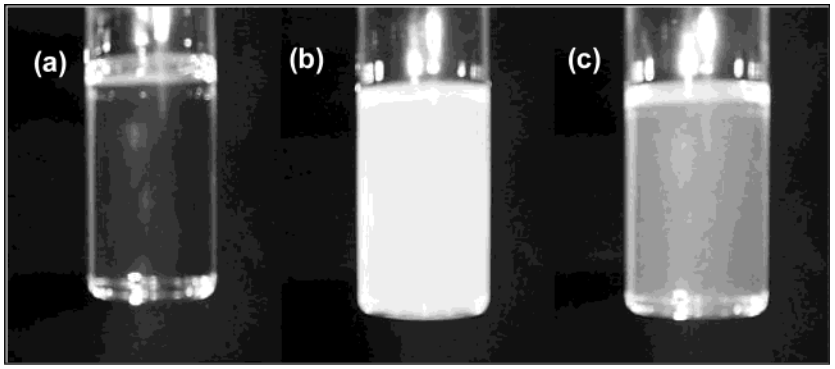

Figure 7. DIP (40%, w/w) was entrapped into 0.5 g L^{-1} micelle solution. (a) At pH 2 DIP solution was transparent. (b) At pH 9−10, DIP was precipitated as yellow fine particles. (c) $MPEG_{113}-DMA_{38}-DEA_{86}$ copolymer solution (pH 2) was mixed with the solution in (b) and micelles were formed because the pH changed to about 9. The yellow precipitate disappeared to give a translucent solution in which the drug was entrapped by the copolymer micelles.

change in the size of the micelles with increasing concentration up to 1.0 g L^{-1}. In contrast, the mean size of the $MPEG_{45}-DMA_{47}-DEA_{120}$ micelles increases significantly, from 33 nm at 0.10 g L^{-1} to 90 nm at 1.0 g L^{-1}, an increase in micelle size of almost 3-fold. This suggested the existence of micelle aggregates, which was confirmed by the observation of turbid solutions at higher copolymer concentration (5 g L^{-1}). The reason for the significant micelle size increase is the higher hydrophobic content (Table 1) in the copolymer. At a given copolymer concentration and temperature, the size and morphology of the micelles is dominated by the hydrophobic/hydrophilic block composition.[23] In the case of $MPEG_{45}-DMA_{47}-DEA_{120}$, the relatively long DEA blocks provide a strong source of hydrophobic−hydrophobic interaction between micelles. As its counterpart, the relatively short hydrophilic PEG_{45} chain (molecular weight 2000) could not provide effective steric repulsion and outweigh to stabilize the formed micelles,[24,25] though it could stabilize the $MPEG_{45}-DMA_{50}-DEA_{95}$ micelle with a relatively short DEA chain. Hence, the $MPEG_{45}-DMA_{47}-DEA_{120}$ copolymers tended to form larger aggregates. Having almost the same DEA block length in $MPEG_{113}-DMA_{38}-DEA_{125}$ copolymer, the long PEG_{113} chains (molecular weight 5 K) greatly improved the micelle stability (increased steric stabilization) and prevented micelles from further aggregation. Thus, the extent of size increasing of $MPEG_{113}-DMA_{38}-DEA_{125}$ micelle were much less remarkable at the present concentration range, from 0.1 to 1.0 g L^{-1}, compared with $MPEG_{45}-DMA_{47}-DEA_{120}$ micelle.

Drug Incorporation into Micelles. DIP was chosen as the model drug. It is a known coronary vasodilator[26] and a coactivator of antitumor compounds.[27] DIP is soluble in water below pH 5.9 because of the protonation of its amine groups. It becomes water-insoluble above pH 5.9 and precipitates as yellow, needle-shaped crystals. Its solubility in water at pH 7 is 1.5×10^{-5} M, and it increases by a factor of 5 at pH 5. In the presence of conventional surfactant micelles, DIP is localized in the hydrophobic core.[28]

Figure 7 illustrates the solubilization of DIP into $MPEG_{113}-DMA_{38}-DEA_{86}$ micelles. The same behavior was also observed with the three other copolymers (not shown). When DIP was dissolved in water at pH 2, it formed a transparent yellow solution, see Figure 7a. As the pH was raised to above pH 5.9 (pH 10 in this case) by adding 2 M NaOH, the DIP precipitated as fine particles within one minute, and the solution became cloudy yellow (see Figure 7b). On addition of unimeric copolymer solution, the yellow DIP precipitate quickly disappeared, and the copolymer−drug solution became translucent as shown in Figure 7c. The final pH was about pH 9. As demonstrated in Figure 2, MPEG−DMA−DEA unimers aggregated to form micelles in response to the pH shift from pH 2 to 10. These micelles provided hydrophobic microdomains which solubilize small organic molecules, such as DIP, either in a molecular or nanocrystalline state. Along with the partitioning study, the redissolution of the DIP precipitate is strong evidence for the incorporation of DIP into the micelles. However, the actual physical state of the drug within the micelles, and its distribution between micellar core and corona area, remains unclear. These need to be clarified in future studies.

For DLS, TEM, and release studies, a premixed drug−unimer solution with known concentration at low pH was mixed with several drops of 2 M NaOH solution, so that its pH was raised directly to 9. In this way, micellization and DIP entrapment occurred simultaneously.

Further analyses of the DIP solubilization in MPEG−DMA−DEA micelles and the loss of DIP over time were carried out using DLS. The drug contents of micelle solutions were measured by both UV and fluorescence spectroscopy. Table 3 gives the micelle parameters measured by DLS in the absence of DIP. Table 4 gives data for the same micelles loaded with DIP. At the beginning of the experiment, partitioning of the DIP leads to an equilibrium between a saturated solution of DIP in water and the much more concentrated material in the micelle core, in which the free energy of the DIP is much lower. However, if crystallization from the saturated DIP solution occurs, then there is an even lower free energy state available. Thus, during these experiments, the DIP is slowly released from the micelles and precipitates as yellow crystals. These were filtered off before DLS, UV, or fluorescence measurements and DLS measurements were made 24 h after preparation of the micellar solution then again after leaving the solution to stand for 5 days. It was assumed that there was no copolymer loss during drug precipitation.

DLS characterization of the drug-loaded micelles after passing through a 0.45 μm filter indicated reasonably narrow size distributions. For example, the DLS results for $MPEG_{45}-$

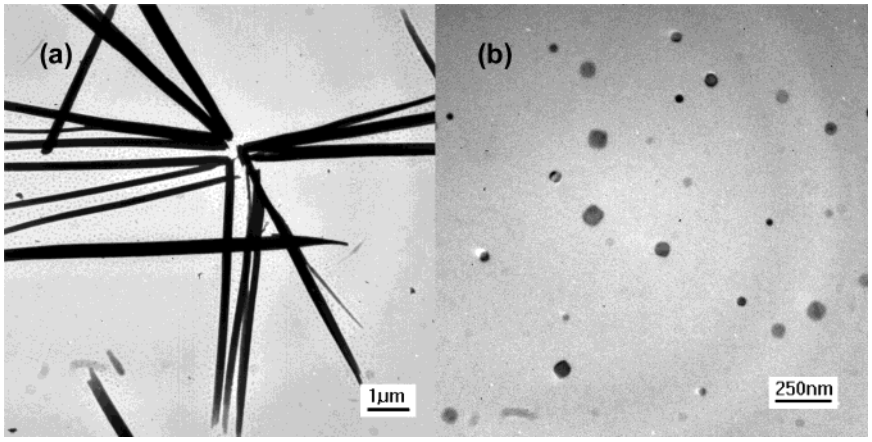

Figure 8. TEM images of drug-loaded micelles made at pH 9 and deposited on copper grid. (a) Crystalline DIP precipitated from basic solution. (b) $MPEG_{45}-DMA_{50}-DEA_{95}$ loaded with 20% (w/w) of DIP.

Table 3. Micelle Parameters from DLS Measurements[a]

	eff. diameter (nm)	polydispersity	scattering intensity (kcps)
$MPEG_{45}-DMA_{47}-DEA_{120}$	56.4 ± 6.5	0.105 ± 0.030	124.0 ± 15.0
$MPEG_{45}-DMA_{50}-DEA_{95}$	32.7 ± 3.0	0.103 ± 0.050	21.9 ± 2.0
$MPEG_{113}-DMA_{40}-DEA_{125}$	42.3 ± 5.0	0.089 ± 0.040	71.2 ± 15.0
$MPEG_{113}-DMA_{38}-DEA_{86}$	30.0 ± 3.0	0.180 ± 0.080	13.2 ± 1.0

[a] Copolymer concentration: 0.5 g L^{-1}, pH 9.

$DMA_{50}-DEA_{95}$ and $MPEG_{113}-DMA_{40}-DEA_{125}$ micelles loaded with DIP at pH 9 (see Table 4) indicated hydrodynamic diameters of 40 and 92 nm, with polydispersities of 0.076 and 0.197, respectively. These results were obtained 24 h after drug loading; similar results were also obtained after 5 days (see below). Comparing Tables 3 and 4, the hydrodynamic diameters of drug-loaded micelles increased by 8−40 nm compared with the empty micelles. The increase in micelle size due to the solubilized drug has been predicted by a recent mathematical simulation of drug solubilization.[10b] Comparison of the drug contents for the three types of copolymer micelles after 1 day and 5 days of storage indicated almost the same amount of drug loading in each micelle, which is consistent with the similar hydrophilic/hydrophobic balance in these copolymers. Although the PEG5000-based copolymer has a lower DEA content (50 mol. %) than the $MPEG_{45}-DMA_{50}-DEA_{95}$ copolymer (see Table 1), the higher drug loading capacity achieved using the longer PEG5000 block compensates for the lower hydrophobic DEA content, so it is reasonable to conclude that these drug-loadings are comparable from a structural point of view.

During storage of the drug-loaded micelle solutions for 5 days, DIP was gradually released as a precipitate and the drug content was reduced from an initial loading of about 20% to around 4−5% (Table 4). This controlled release of the drug from the micelle cores shows that the entrapped DIP is thermodynamically unstable relative to the precipitated DIP. Essentially, the drug-loaded micelles are kinetically stable and thermodynamically unstable. Drug release is driven by the change in chemical potential of the DIP. Meanwhile, the micelle sizes of the three drug-loaded micelles decreased, as expected, because of the drug loss from the cores. However, the size decreases are not comparable: $MPEG_{45}-DMA_{50}-DEA_{95}$ and $MPEG_{113}-DMA_{40}-DEA_{125}$ micelles only showed small size changes. At present we do not have a convincing explanation for these data. At the same time, the intensity of scattered light from the micelles also decreased, which can be explained as being due to a decrease in the density, and hence refractive index, of the drug-loaded micelles. Loss by precipitation is completely reversible in the sense that cycling the pH back to acidic will rehomogenize the drug/unimers solution and rapid return to high pH regenerates drug-loaded micelles.

Morphology of DIP Loaded Micelles. MPEG−DMA−DEA micelles have previously been shown to be spherical,[16] whereas precipitated DIP crystals (obtained by adding NaOH to an acid DIP solution) are needle-shaped. Figure 8 shows TEM images of precipitated DIP prepared in the absence of any copolymer and of DIP-loaded $MPEG_{45}-DMA_{50}-DEA_{95}$ micelles. Even at 20% DIP loadings, the micelles remained spherical, and no needle-shaped morphology was observed. The mean micelle diameters ranged from 30 to 100 nm, which is consistent with the results obtained from DLS measurements for the same micelles, especially considering the dry state of the micelles in the conditions of the TEM experiment and taking into account polydispersity effects.

Drug Release from Micelles. The drug release from MPEG−DMA−DEA micelles was measured by the in situ UV cuvette setup shown in Figure 1. In this method, 3.0 g

Table 4. Sizes and Stability of DIP-Loaded Micelles[a]

	eff. diameter (nm)		polydispersity		scattering intensity (kcps)		drug content (w/w %)[b]	
copolymers	one day	five days	one day	five days	one day	five days	one day	five days
$MPEG_{45}-DMA_{47}-DEA_{120}$	60	59	0.076	0.071	152.2	120.9	18.5	10.0
$MPEG_{45}-DMA_{50}-DEA_{95}$	40	39	0.076	0.075	35.5	25.0	15.6	4.8
$MPEG_{113}-DMA_{40}-DEA_{125}$	92	89	0.197	0.194	157.7	103.2	17.3	5.0
$MPEG_{113}-DMA_{38}-DEA_{86}$	67	54	0.265	0.238	49.4	24.6	16.5	4.4

[a] 20% (w/w) of DIP loaded in the micelles with a concentration of 0.5 g L^{-1}. [b] Drug content measured by UV spectroscopy in pH 3 buffer, 284 nm.

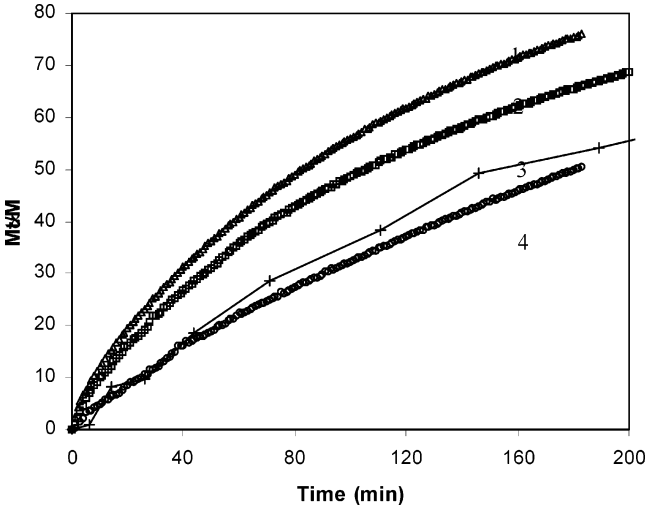

Figure 9. Cumulative DIP release to environments of varying pH at 37 °C. In the blank release (curve 1), 0.01 g, 1 g L^{-1} DIP solution without micelles at pH 3 was released to 3.0 g of pH 3 buffer solution. 20% of DIP entrapped in 0.5 g L^{-1} $MPEG_{45}-DMA_{50}-DEA_{95}$ micelle solution (prepared at pH 9) was released to pH 7.4 buffer (curve 4) and pH 3 buffer (curve 2), respectively. A comparison was made with 5 mL of 0.5 g L^{-1} of micelle entrapped 20% DIP released to 50 mL of PBS buffer, pH 7.4 (curve 3).

of external PBS buffer in the quartz cuvette was used as a release medium and 0.09 g of DIP-loaded $MPEG_{45}-DMA_{50}-DEA_{95}$ micelle solution was the release source. The medium-to-sample ratio was about 100:3, which is comparable to conventional methods using dialysis bags for drug release experiments. Figure 9 shows typical results. This in situ setup mimics the conventional dialysis bag method and has been checked by a parallel experiment using the conventional method for comparison. A dialysis bag with 5 mL of 20% entrapped DIP in 0.5 g L^{-1} $MPEG_{45}-DMA_{50}-DEA_{95}$ micelle solution was hung in 50 mL of PBS buffer solution, and 1 mL of the external solution was withdrawn for UV spectroscopy analysis after defined intervals. From Figure 9, these two methods (curves 3 and 4) give similar release results, indicating the reliability of this in situ measurement and its consistency with the conventional method. In both experiments, data were collected and analyzed only over the first 3 h, to ensure a sink condition.

Because of the low solubility of DIP at the pH of the micellar solutions, a blank release experiment (curve 1 in Figure 9) for DIP without micelles was performed at pH 3. using an equivalent amount of drug (1.98×10^{-3} M) to that trapped in the micelle solution. It is assumed that the DIP diffusion rate in the buffer solution did not change with the solution pH. This experiment measures the permeation of the DIP through the dialysis membrane in the absence of any control by the micelles.

From Figure 9, the comparison between the blank and micellized drug release demonstrated that drug release from micelles in a pH 7.4 buffer (curve 3 and 4) was slower than the drug alone dissolved in a pH 3 buffer (curve 1). After 1 h, the cumulative curves showed that about 40% of DIP was released in the absence of micelles, which was twice as high as the DIP released from the micelles. This retardation effect on the rate of DIP diffusion demonstrated the controlled release properties of the MPEG−DMA−DEA micelles.

It has been shown that MPEG−DMA−DEA micelles dissociate below pH 7. Given the greatly increased solubility of DIP at low pH, this pH-triggered micellar dissociation suggests that fast, triggered release of DIP should be feasible. To investigate this possibility, a DIP-loaded micelle solution was prepared at pH 9 and was then placed in a pH 3 buffer. As shown in Figure 9, its release (curve 2) was only slightly slower than the blank drug release (curve 1) but was faster than the drug release rate at pH 7.4 (curve 4). The slightly retarded release rate is related to the protonation of the DEA block and DIP in acid media, followed by micelle dissociation and drug release. Therefore, the comparatively fast pH-triggered release indicated that MPEG−DMA−DEA micelles have some potential for controlled drug release. Further work on the effect of copolymer composition on controlled release profiles are in progress.

Conclusions

Amphiphilic MPEG−DMA−DEA triblock copolymers can be synthesized in mild conditions with good control over molecular weight and block length by using ATRP. The polymers can be molecularly dissolved in acidic aqueous media at room temperature. As the pH is raised above 7, spontaneous self-assembly into micelles occurs, in which the water-insoluble DEA blocks form the hydrophobic cores, and MPEG and DMA form the coronas and inner shells, respectively.

Dipyridamole, a model drug that dissolves in acid but is insoluble above pH 5.8, was loaded into these micelles by rapidly changing the pH of the copolymer/drug solution from 2 to 8. This protocol has the advantage of needing no organic solvent. Fluorescence studies of both pyrene and DIP confirmed efficient partitioning of these molecules into the micelle cores at high pH.

The dynamic light scattering measurement indicated that the diameters of micelles formed in the presence of DIP ranged from 20 to 90 nm, depending on the block composition, copolymer concentration and drug loading. Larger micelles were obtained from copolymers with longer hydrophobic blocks. Conversely, longer hydrophilic MPEG blocks led to smaller micelles due to the increased hydrophilic character of the copolymer chains. The drug-loaded micelles were bigger than the empty micelles, as expected. DLS studies indicated that the light scattering intensities from DIP-loaded micelles decreased as the drug was lost from these micelles.

Storage of drug-loaded micelle solutions leads to slow release of the DIP, over a period of days, driven by precipitation of the soluble component of the drug in equilibrium with the micelles. Drug release profiles obtained by monitoring diffusion through a membrane using in situ UV spectroscopy indicated that the DIP in the MPEG−DMA−DEA micelles can be slowly released into a surrounding solution with no drug in it if the solution pH is maintained at around 7.4. Rapid, triggered release results when the solution pH is switched to 3, to dissociate the micelles. Thus, these reversible micelle systems offer potential both for both controlled and pH-triggered drug

release. Their main advantages are the very easy synthesis of the ABC triblock copolymers, which can be performed in aqueous solution at room temperature, the possibility of producing drug loaded micelles without any cosolvent and the potential for shell cross-linking.

Acknowledgment. This work was supported by a grant from the Engineering and Physical Sciences Research Council, which the authors gratefully acknowledge.

References and Notes

(1) (a) Torchilin, V. P. *J. Controlled Release* **2001**, *73*, 137. (b) Kwon, G. S.; Kataoka, K. *Adv. Drug Delivery Rev.* **1995**, *16*, 295. (c) Allen, C.; Maysinger, D.; Esienberg, A. *Colloids Surf. B: Biointerfaces* **1999**, *16*, 3. (d) Forster, S.; Plantenberg, T. *Angew. Chem., Int. Ed.* **2002**, *41*, 688.

(2) Wang, Y. L.; Banziger, J.; Dubin, P. L.; Filippelli, G.; Nuraje, N. *Environ. Sci. Technol.* **2001**, *35*, 2608.

(3) (a) Harada, A.; Kataoka, K. *Macromolecules* **1998**, *31*, 288. (b) Harada, A.; Kataoka, K. *J. Controlled Release* **2001**, *72*, 85.

(4) Gref, R.; Domb, A.; Quellec, P.; Blunk, T.; Müller, R. H.; Verbavatz, J. M.; Langer, R. *Adv. Drug Delivery Rev.* **1995**, *16*, 215.

(5) (a) Kabanov, A. V.; Chekhonin, V. P.; Alakhov, V. Yu.; Batrakova, E. V.; Lebedev, A. S.; Melik-Nubarov, N. S.; Arzhakov, S. A.; Levashov, A. V.; Morozov, G. V.; Severin, E. S.; Kabanov, V. A. *FEBS Lett.* **1989**, *258*, 343. (b) Kabanov, A. V.; Nazarova, I. R.; Astafieva, I. V.; Batrakova, E. V.; Alakhov, V. Yu.; Yaroslavov, A. A.; Kabanov, V. A. *Macromolecules* **1995**, *28*, 2303. (c) Marin, A.; Muniruzzaman, M.; Rapoport, N *J. Controlled Release* **2001**, *75*, 69.

(6) (a) Nah, J. W.; Jeong, Y. I.; Cho, C. S. *J. Polym. Sci.: Part B: Polym. Phys.* **1998**, *36*, 415. (b) Jeong, Y. I.; Cheon, S. H.; Kim, S. H.; Nah, J. W.; Lee, Y. M.; Sung, Y. K.; Akaike, T.; Cho, C. S. *J. Controlled Release* **1998**, *51*, 169.

(7) Kwon, G.; Naito, M.; Yokoyama, M.; Okano, T.; Sakurai, Y.; Kataoka, K. *J. Controlled Release* **1997**, *48*, 195.

(8) (a) Kim, S. Y.; Ha, J. C.; Lee, Y. M. *J. Controlled Release* **2000**, *65*, 345. (b) Kim, S. Y.; Shin, I. G.; Lee; Y. M.; Cho, C. S.; Sung, Y. K. *J. Controlled Release* **1998**, *51*, 13.

(9) Chung, J. E.; Yokoyama, M.; Aoyagi, Y.; Sakurai, T.; Okano, T. *J. Controlled Release* **1998**, *53*, 119.

(10) (a) Nagarajan, R.; Ganesh, K. *Macromolecules* **1989**, *22*, 4312. (b) Xing, L.; Mattice, W. L. *Langmuir* **1998**, *14*, 4074.

(11) Martin, T. J.; Prochazka, K.; Munk, P.; Webber, S. E. *Macromolecules* **1996**, *29*, 6071.

(12) (a) Gohy, J. F.; Antoun, S.; Jérôme, R. *Macromolecules* **2001**, *34*, 7435. (b) Gohy, J. F.; Varshney, S. K.; Jérôme, R. *Macromolecules* **2001**, *34*, 3361.

(13) Vamvakaki, M.; Billingham, N. C.; Armes, S. P. *Macromolecules* **1999**, *32*, 2088.

(14) (a) Bütün, V.; Armes, S. P.; Billingham, N. C. *Polymer* **2001**, *42*, 5993. (b) Bütün, V.; Billingham, N. C.; Armes, S. P. *Chem. Commun.* **1997**, 671. (c) Bütün, V.; Wang, X.-S.; de Paz Banez, M. V.; Robinson, K. L.; Billingham, N. C.; Armes, S. P. *Macromolecules* **2000**, *33*, 1.

(15) Liu, S.; Armes, S. P. *Curr. Opinion Colloid & Interface Sci.* **2001**, *6*, 249.

(16) Liu, S.; Weaver, J. V. M.; Tang, Y.; Billingham, N. C.; Armes, S. P.; Tribe, K. *Macromolecules* **2002**, *35*, 6121.

(17) (a) Borisevitch, I. E.; Tabak, M. *J. Luminescence* **1992**, *51*, 315. (b) Tabak, M.; Borisevitch, I. E. *Biochim. Biophys. Acta* **1991**, *241*, 1116.

(18) (a) Wang, X.-S.; Armes, S. P. *Macromolecules* **2000**, *33*, 6640. (b) Bütün, V.; Lowe, A. B.; Billingham, N. C.; Armes, S. P. *J. Am. Chem. Soc.* **1999**, *121*, 4288.

(19) Lee, A. S.; Gast, A. P.; Bütün, V.; Armes, S. P. *Macromolecules* **1999**, *32*, 4302.

(20) Wilhelm, M.; Zhao, C.-L.; Wang, Y.; Xu, R.; Winnik, M. A.; Mura, J. -L.; Riess, G.; Croucher, M. D. *Macromolecules* **1991**, *24*, 1033.

(21) Kalyanasyndaram, K. *Photochemistry in Microheterogeneous Systems*; Academic Press: New York, 1987.

(22) Kozlov, M. Yu.; Melik-Nubarov, N. S.; Batrakova, E. V.; Kabanov A. V. *Macromolecules* **2000**, *33*, 3305.

(23) Förster, S.; Zizenis, M.; Wenz, E.; Antonietti, M. *J. Chem. Phys.* **1996**, *104*, 9956.

(24) La, S. B.; Okano, T.; Kataoka, K. *J. Pharm. Sci.* **1996**, *85*, 85.

(25) Allen, C.; Yu, Y.; Maysinger, D.; Eisenberg, A. *Bioconjugate Chem.* **1998**, *9*, 564.

(26) Marchandt, E.; Prichard, A. D.; Casanegra, P.; Lindsay, L. *Am. J. Cardiol.* **1984**, *53*, 718.

(27) Shalinsky, D. R.; Jekunen, A. P.; Alcaraz, J. E.; Christen, R. D.; Kim, S.; Khatibi, S.; Howell, S. B. *Brit. J. Cancer* **1993**, *67*, 30.

(28) Borisevitch, I. E.; Borges, C. P. F.; Yushmanov, V. E.; Tabak, M. *Biochim. Biophys. Acta* **1995**, *1238*, 57.

BM030026T